tion, avoiding gene-cloning steps, and investigators can obtain initial measures of binding affinity while the protein is displayed on the yeast surface. This obviates the need to individually purify 73 different proteins. And after biophysical characterization of the two binders, the yeast are then used for a selection process called affinity maturation. The effectiveness of this experimental workflow may pave the way for future efforts to test computationally designed protein interactions.

Another possible reason for their achievement involves the computational design protocol. Previous modest-affinity binders were developed by focusing first on the placement of the two proteins, and then on high-resolution all-atom side chain design (*9*, *10*). Fleishman *et al.* took a different approach. They first focused on all-atom placement of disembodied side chains to establish critical "hot spot" interactions, and then on docking the designed protein to its target. This strategy is reminiscent of a previous approach that involved grafting key residues from a known interaction onto a new protein scaffold to generate a new binding pair (*13*). If there are no known hot spot binding motifs, however, these hot spot interactions must be designed de novo (*1*).

To create tight binders (dissociation constant < 50 nM) from their initial hits (apparent affinities of >2000 nM and >5000 nM), Fleishman *et al.* performed affinity maturation with yeast display. An examination of the stabilizing mutations suggested ways of improving their computational methods; for instance, the authors concluded that future modeling efforts should try to take into account subtle movements of sequence backbones, attractive forces known as long-range electrostatics, and the energy costs associated with protein interactions (such as the desolvation cost for "burying" polar atoms). Optimizing a protein energy function, however, presents a challenge, and the insights gained from this single study will need to be combined with results from other design and modeling studies in order to identify robust improvements.

Although Fleishman *et al.* have produced a landmark result, it is evident that computational protein interface design is not a solved problem. Researchers should not be satisfied with one or a few successes in solving these astronomically complex molecular puzzles. Each new puzzle is different from the last; for example, the region of hemagglutinin targeted in this work was hydrophobic and α-helical. Will the computational protocol developed by Fleishman *et al.* also be effective for designing binders for polar surface patches, or targeting alternative secondary structures (see the figure) such as β sheets, strands, or loops? Creating many of these interfaces will require accurate modeling of protein conformations and accurate evaluation of desolvation, electrostatics, and hydrogen bonding.

The endeavor to understand protein interactions will undoubtedly continue for decades to come. And the pursuit should remain persistent, as the impacts of rational design and manipulation of protein-protein interactions can hardly be overstated.

References

1. S. J. Fleishman *et al.*, *Science* **332**, 816 (2011).
2. D. J. Mandell, T. Kortemme, *Nat. Chem. Biol.* **5**, 797 (2009).
3. J. Karanicolas, B. Kuhlman, *Curr. Opin. Struct. Biol.* **19**, 458 (2009).
4. A. Leaver-Fay *et al.*, *Methods Enzymol.* **487**, 545 (2011).
5. S. S. Sidhu, S. Koide, *Curr. Opin. Struct. Biol.* **17**, 481 (2007).
6. I. A. Wilson, N. J. Cox, *Annu. Rev. Immunol.* **8**, 737 (1990).
7. D. C. Ekiert *et al.*, *Science* **324**, 246 (2009).
8. J. Sui *et al.*, *Nat. Struct. Mol. Biol.* **16**, 265 (2009).
9. P.-S. Huang *et al.*, *Protein Sci.* **16**, 2770 (2007).
10. R. K. Jha *et al.*, *J. Mol. Biol.* **400**, 257 (2010).
11. J. Karanicolas *et al.*, *Mol. Cell* **42**, 250 (2011).
12. S. A. Gai, K. D. Wittrup, *Curr. Opin. Struct. Biol.* **17**, 467 (2007).
13. S. Liu *et al.*, *Proc. Natl. Acad. Sci. U.S.A.* **104**, 5330 (2007).

10.1126/science.1207082

PHYSICS

Brownian Motion Goes Ballistic

Measurements of the Brownian motion of particles in air and in water reveal a smooth "ballistic" motion at very short times.

Peter N. Pusey

When Einstein explained the origin of Brownian motion in 1905, he described the erratic movement of a microscopic particle driven by the thermal motion of liquid molecules as a random walk with sharp changes of direction between each step (*1*). He realized that this picture—the one we seem to see if we watch a particle under the microscope—must break down if we were to look more closely. A moving object would require an infinite force to change its speed or direction discontinuously. The particle actually moves "ballistically" along a smooth trajectory (*2*–*4*), as if it were a microscopic ocean liner on an erratic course (see the first figure, panels A and B). It has taken more than a century to observe this ballistic motion. The studies of Li *et al.* (*5*) were conducted on particles in air; its low viscosity allowed ballistic motion to be followed accurately for extended periods and showed that a particle's instantaneous velocities along its path obey a statistical distribution consistent with thermal motion. Huang *et al.* (*6*) used liquid water; in this higher-density medium, the transition from ballistic motion at short times to diffusive motion at longer ones could be studied in detail.

Einstein estimated (*2*–*4*) that a particle of diameter 1 μm in water would move for only about 0.1 μs over a distance of only about 2 Å before completely changing its speed and direction. The minute magnitudes of these estimates led Einstein to conclude that only the larger-scale diffusive random walk would be observed in practice. The present experiments used technologies undreamed of in Einstein's time. Single particles were held in optical traps—radiation pressure prevents them from settling under gravity. A fast position-sensitive detector (*7*) split the interference pattern formed between light scattered by the particle and the trapping laser beam itself and fed the two parts to two photodiode detectors. Lateral motion of a particle in the trap increases the intensity at one detector but decreases it at the other. The difference between the two signals measures one component of the particle's position. Coupled to fast electronics, this system can measure displacements as small as 0.3 Å in time intervals as short as 0.01 μs.

In a vacuum, a particle in an optical trap would oscillate indefinitely. Gas molecules both dampen the oscillations and introduce random impulses that induce Brownian motion. Li *et al.* determined the time evolution of the position and velocity of a 3-μm-diameter silica sphere trapped in air at about 1/36 of atmospheric pressure (see the second figure, panel A). The underlying oscillatory motion, with a period of about 300 μs, is evident, as is a degree of randomness induced by the gas molecules. Einstein (*2*–*4*) estimated the duration of ballistic Brownian motion to be the time $\tau_p = m/\gamma$

SUPA, School of Physics, University of Edinburgh, Edinburgh EH9 3JZ, UK. E-mail: p.n.pusey@ed.ac.uk

over which the particle's velocity would decay through friction with the gas (or liquid), if the random impulses from its molecules were neglected; here m is the particle's mass and γ is its Stokes friction coefficient that describes drag (*8*, *9*). For the experiment of Li *et al.*, $\tau_p \approx 150$ μs, so that random changes in the velocity occurred on a time scale similar to that of the coherent oscillations (the motion is underdamped).

Li *et al.* constructed histograms of the instantaneous velocities at air pressures of both 1/36 and 1 atm, where the particle's velocity changed more rapidly ($\tau_p \approx 50$ μs). These were accurately described by the Maxwell-Boltzmann distribution with a root-mean-square (rms) velocity of about 0.42 mm/s, in good agreement with the theoretical value from equipartition of energy for conditions of thermal equilibrium [$v_{rms} = (k_B T/m)^{1/2}$, where k_B is the Boltzmann constant and T the temperature]. Li *et al.* also showed that the particle's mean-square displacement (MSD, a measure of average distance traveled) agreed well with old calculations of underdamped Brownian motion in a harmonic potential (*10*).

In a liquid, the duration of a Brownian step, $\tau_p \approx 0.1$ μs, is much smaller than the natural oscillation period of the trap, making the motion strongly overdamped. Although it is more difficult to access the ballistic regime itself, experimental studies in liquids enable a detailed examination of the transition from ballistic to diffusive motion. Huang *et al.* measured the MSD of a 1-μm-diameter silica sphere in water (*11*) (see the second figure, panel B). At the shortest times ($t \approx 0.01$ to 0.03 μs), the MSD increases as t^2 (a line of slope 2 in the double logarithmic plot), which corresponds to ballistic motion. Between roughly 2 μs < t < 20 μs, the particle makes many random steps, and the MSD increases as t, which is characteristic of diffusion (*11*). The particle's free diffusion is finally limited by the trapping potential, causing the MSD to saturate at t > 100 μs.

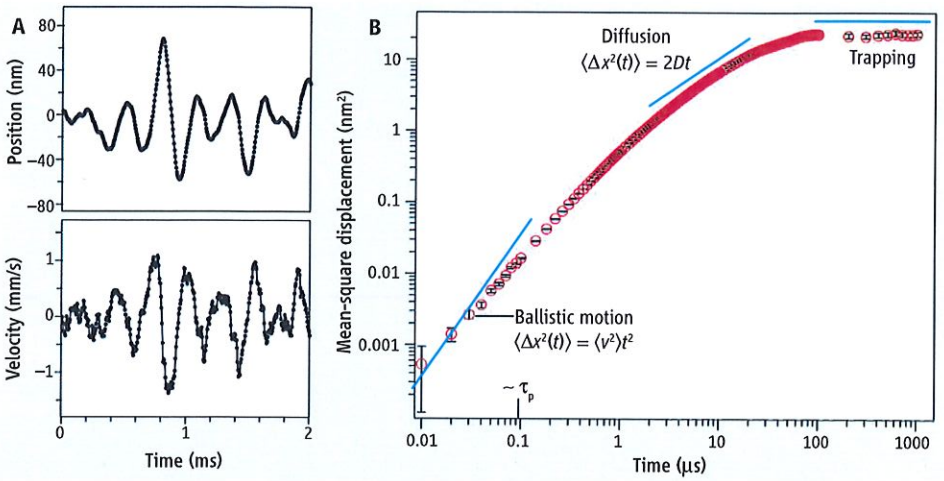

Resolving ballistic motion. (**A**) Li *et al.* measured the position and velocity of a 3-μm-diameter silica sphere optically trapped in air at about 1/36 of atmospheric pressure. Oscillations in the underdamped motion were randomly perturbed by collisions with the gas molecules. (**B**) Huang *et al.* measured the mean-square displacement of a 1-μm-diameter silica sphere trapped in water, which displayed the slow transition from ballistic to diffusive Brownian motion. Note the remarkable resolution of the measurement: 0.001 nm² corresponds to a displacement of 0.3 Å, measured in about 0.02 μs. [Panel B adapted from (*6*)]

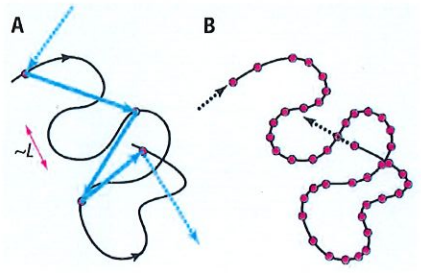

Timing is everything. (**A** and **B**) A particle undergoing Brownian motion is buffeted at random by thermally agitated fluid molecules, and it follows a tortuous but locally smooth path (black line). It loses memory of its speed and direction over the very small distance ~L. What an observer actually sees depends on the resolution of the position measurement. In the case considered by Einstein (**A**), the particle's speed and direction have changed many times between measurements (the red dots), and the observer sees a diffusive random walk with uncorrelated steps (the blue arrows). Measurements made at shorter time intervals (**B**) resolve the smooth ballistic motion.

For many years after Einstein's contributions, it was expected that the transition from ballistic to diffusive motion would be quite sharp, corresponding to an exponential decay of the particle's memory of its earlier velocity. However, about 50 years ago, hints from computer simulations and theory started to suggest a more complex scenario. In particular, hydrodynamic vortices in the liquid created by the particle's motion lead to memory effects, and the particle's velocity decays much more slowly than exponentially, exhibiting a $t^{-3/2}$ "long-time-tail" (*12*). Detailed analysis by Huang *et al.* of data like that shown in the second figure, panel B, where the ballistic-to-diffusive transition spans more than three decades in time, has now provided a thorough verification of the full, complicated hydrodynamic theory (*13*, *14*). Although several previous experiments had observed the breakdown of the simple diffusion picture [e.g., (*15*)], the present studies extend into the ballistic regime.

What next? Li *et al.* mention the fascinating prospect of laser cooling a trapped particle to a temperature at which quantization of the energy of this mesoscopic object could be observed (*16*). Huang *et al.* suggest extending their measurements to Brownian motion in confined regions and heterogeneous media. Here, understanding the details of prediffusive motion over subnanometer distances could well be relevant to some biological processes, such as the lock-and-key mechanism of enzyme action.

References and Notes

1. A. Einstein, *Ann. Phys.* **322**, 549 (1905).
2. A. Einstein, *Zeit. Elektrochem.* **13**, 41 (1907).
3. Both (*1*) and (*2*) are translated and reprinted in (*4*).
4. A. Einstein, in *Investigations on the Theory of Brownian Movement*, R. Fürth, Ed. (Dover, New York, 1956).
5. T. Li *et al.*, *Science* **328**, 1673 (2010).
6. R. Huang *et al.*, *Nat. Phys.* (2011); 10.1038/nphys1953:arxiv:1003.1980.
7. I. Chavez *et al.*, *Rev. Sci. Instrum.* **79**, 105104 (2008).
8. The Stokes friction coefficient is given by $\gamma = 6\pi\eta R$, with R the particle's radius and η the shear viscosity of the liquid. At low pressure, where the mean-free path of a gas molecule is comparable to R, the friction is reduced by a substantial "Cunningham slip correction" (*9*).
9. E. Cunningham, *Proc. R. Soc. A* **83**, 357 (1910).
10. G. E. Uhlenbeck, L. S. Ornstein, *Phys. Rev.* **36**, 823 (1930).
11. In an isotropic random process like Brownian motion, the average velocity and average displacement are zero. The simplest descriptor of average motion is the MSD, the square of $\Delta x(t)$, the distance moved in time t, averaged over many measurements. For ballistic motion (straight line and constant speed) $\langle \Delta x^2(t) \rangle = \langle v^2 \rangle t^2$; for diffusion, Einstein's result is $\langle \Delta x^2(t) \rangle = 2Dt$, with the diffusion constant given by $D = k_B T/\gamma$ (*1*).
12. B. J. Alder, T. E. Wainwright, *Phys. Rev. A* **1**, 18 (1970).
13. E. J. Hinch, *J. Fluid Mech.* **72**, 499 (1975).
14. H. J. H. Clercx, P. P. J. M. Schram, *Phys. Rev. A* **46**, 1942 (1992).
15. B. Lukic *et al.*, *Phys. Rev. Lett.* **95**, 160601 (2005).
16. T. Li *et al.*, *Nat. Phys.* (2011); 10.1038/nphys1952.

10.1126/science.1192222